FP7 Collaborative Project

CLARIS LPB

A Europe-South America Network for Climate Change Assessment and Impact Studies in La Plata Basin

http://www.claris-eu.org

Instrument : **FP7 Collaborative Project**

Thematic Priority: **Priority Area 1.1.6.3 "Global Change and Ecosystems"**

D9.4: Characterization of decadal variability of river discharges for hydropower production in the basin, including its spatial and seasonal dependence and its long term variability.

Due date of deliverable: Month 18

Start date of project: **01/10/2008** Duration: 4 **years**

Organisation name of lead contractor for this deliverable: **UR**

Deliverable No	Deliverable title	WP	Lead beneficiary	*Estimated indicative person-months (permanent staff)*	Nature	Dissemination level	Delivery date
D9.4	Characterization of decadal variability of river discharges for hydropower production in the basin, including its spatial and seasonal dependence and its long term variability.	WP9	P17-UR	2,50	R	PU	18

1. Introduction

Hydroelectric energy in La Plata Basin (LPB) has a relatively low cost and a very large share of the energy supply. However, water availability in dams presents a large uncertainty, particularly in the various multi-annual time scales, hindering long-term energy planning. Previous studies suggest the existence of multi-annual oscillations and long-term trends in the regional climate. These patterns show a certain degree of regularity that provides a good opportunity to reduce the uncertainty of water supply, contributing to better decision-making and risk management processes.

Robertson and Mechoso (1998) analyzed for the period 1911-1993 the annual time series of the mean of: 1) Uruguay-Negro and 2) Paraguay-Paraná rivers (previously normalized by their respective standard deviations). The former show predominant variabilities both at El Niño-Southern Oscillation (ENSO) and lower frequency time scales, i.e., around 2.5-5 and 6 years respectively. The latter exhibit a non-linear trend and a near-decadal component (around 9 years). In this work, Negro, Uruguay and Paraná rivers are considered individually and their multi-annual variabilities are analyzed both for the annual and seasonal streamflow. Data and methods are described in Sections 2 and 3 respectively. Section 4 shows the obtained results. The study is concluded in Section 5.

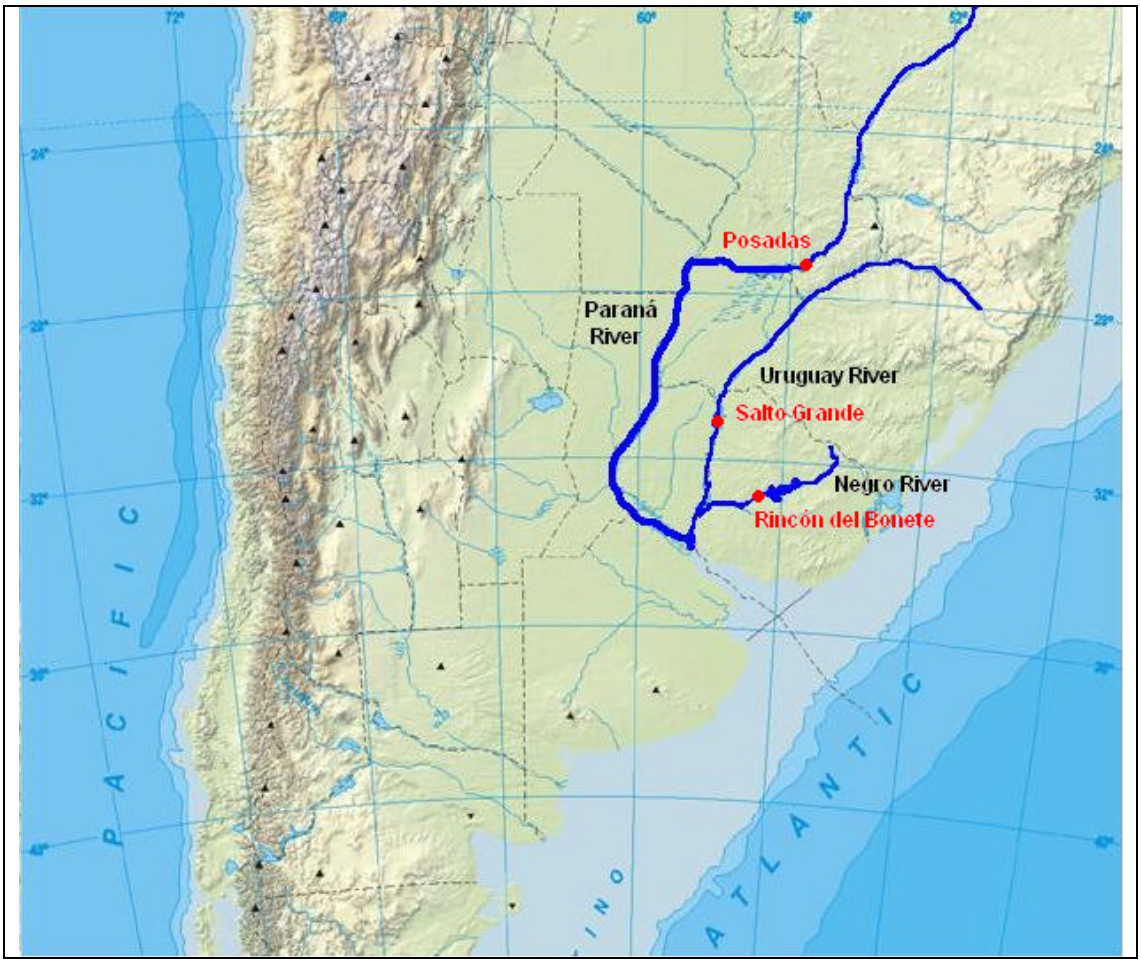

Figure 1.-Location of the discharge gauge stations for the three rivers selected in this study.

2. Data

The data used in this study are monthly streamflow of the following rivers: Negro (1908-2007), Uruguay (1909-2007) and Paraná (1901-1999), measured at Rincón del Bonete dam, Salto Grande dam and Posadas, respectively (see Fig. 1). Annual and overlapping three-monthly series are analyzed in order to study both the annual and seasonal variabilities. Furthermore, for the purpose of finding potential links between the streamflow and the global climate, monthly series of Niño 3.4 (1900-2007) and Pacific Decadal Oscillation (PDO, 1900-2008) indices are also analyzed. In these cases, annual series are mostly used and the record periods were chosen to fit with those of the river data.

For the annual series, Negro and Uruguay rivers are considered on a calendar basis, while for Paraná and both global climatic indices years are defined from September to August or from August to July respectively. These differences are due to the interest of having the period of maximum amplitude of river discharges at the middle of the cycle.

3. Methods

Detection of dominant variability modes in multi-annual scales for climatic series has been addressed through modern methods of time series analysis. Singular spectrum analysis (SSA) (Vautard et al., 1992; Ghil et al., 2002) allows to extracting information from relatively short and noisy time series, as those usually appearing in geophysics. Given a time series with equally time-spaced data (one year in this work), SSA decomposes it in three types of additive components: pseudo-periodic (or quasi-periodic) oscillatory patterns, low frequency variability (LFV) modes, and noise. The oscillatory components may be modulated in phase and amplitude. The LFV modes are usually called “trends”, but as this word is commonly associated to increasing or decreasing patterns, which need not be the case, we will restrict its use for this latter sense, in order to avoid confusions.

A difference between SSA and other classic spectral methods is that it does not use prescribed functions (i.e., sines and cosines) but it builds its own data-dependent bases instead. Although SSA will not be described in detail here, some of its aspects will be outlined in order to clarify its applications in this study.

The method involves the choice of a window size (M years). There is no clear-cut rule to select M, so it is advisable to conduct analyses with various values of M. The steadiness of the results is a measure of the robustness of the underlying signal present in the data. In any case, it is recommended that M does not exceed one third of the time series length. It should be considered that, in this context, LFV modes must be understood as displaying significant spectral power only in frequencies lower than 1/M cycles/year (or, equivalently, in periods longer than M years).

One of the stages of the SSA procedure is a principal component problem. The associated eigenvalues (evs) are subjected to a Monte Carlo (MC) statistical significance test in the following way: a first auto-regressive process (AR-1) is adjusted to the given time series and eventually the corresponding evs are calculated. (For the sake of clarity, one can think of the first ev, but the process is done for all of them.) This is done many times (typically 1000 in this study) in order to build a distribution of simulated evs. The percentile occupied by the ev associated to the given time series is then determined, indicating directly the level of significance attained. In this study we will retain those modes for which the corresponding ev is larger than the 95% percentile, and in this case we will say that it is significant at the 90% (two-sided) level. The rationale for comparing the time series to an AR-1 process (or red noise process) is that usually climatic time series show larger spectral power in lower frequencies.

For each ev, SSA builds a reconstructed component (RC) of the same length as the given time series and conserving phase information. The signal-to-noise ratio can be enhanced by a partial

reconstruction of the original series considering RCs associated to significant modes. Besides, RCs, either associated to oscillations or to LFV modes, have the property of being narrowband. For each RC, a characteristic pseudo-frequency is estimated by maximizing the correlation of the associated empirical orthogonal function with a sinusoid.

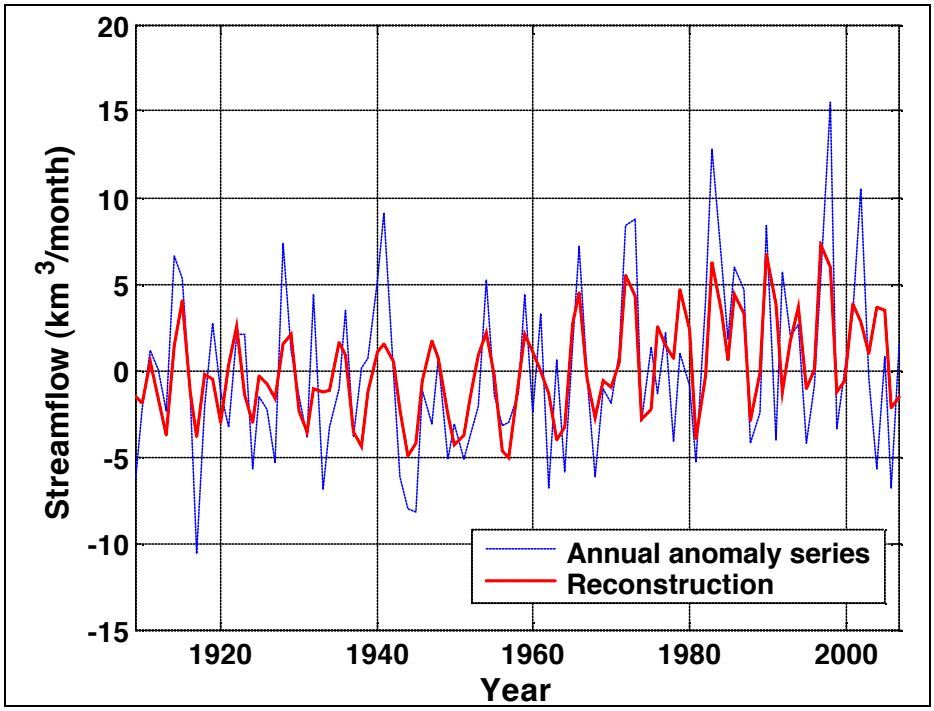

Figure 2.- Annual anomaly time series for Uruguay River and RC associated to the first 5 components obtained using SSA with a window size of M=20 years.

Table 1.- Pseudo-periods associated with each of the first 5 modes of Uruguay River annual series, obtained using SSA with a window size of M=20 years.

Mode	Associated pseudo-period (years)
1	LFV (> 20 years)
2	6.3
3	6.3
4	3.6
5	3.6

As an example, Fig. 2 shows the annual anomaly time series for Uruguay River together with the reconstruction given by the first 5 RCs, for M=20. Table 1 shows the pseudo-period associated to each of the 5 modes. The fraction of explained variance by this reconstruction is 0.349.

A very adequate spectral method for narrowband time series is the maximum entropy method (MEM, Penland et al., 1991; Vautard et al., 1992). When applied to narrowband time series, MEM finds estimates of spectral power avoiding most of the spurious spectral peaks that show up in other methods. MEM is a parametric method for which a statistical significance test has not been developed. Fig. 3 shows the result of applying this method to the RC series shown in Fig. 2.

SSA-MC and SSA followed by MEM (SSA-MEM) have been extensively used in this study. Furthermore, for annual time series additional methods were used in order to assess the robustness of results. These methods are briefly described below.

An alternative method to obtain estimates of the spectrum for a given time series is the Multi-Taper Method (MTM, Vautard et al., 1992; Ghil et al., 2002). This non-parametric method seeks to reduce the variance of spectral estimates, using a small set of "tapers" instead of only one, as in classic methods. Tapers are built so as to minimize the spectral leakage due to the finite length of the series. The method has been modified by Mann and Lees (1996), taking into account the above mentioned feature of geophysical time series, i.e. that they tend to concentrate spectral power in lower frequencies.

Another relatively modern method for time series analysis is wavelet analysis (WA, Torrence and Compo, 1998). This is an appropriate tool for non-stationary time series presenting multiple timescales and occurring in finite temporal domains. One of the advantages of WA over classic spectral methods is that although it uses predetermined function bases, it is designed not only to identify significant

oscillations having dominant periods but also to localize temporally its occurrence. WA has been utilized to identify dominant periods in streamflow time series of major rivers around the world (Labat, 2008).

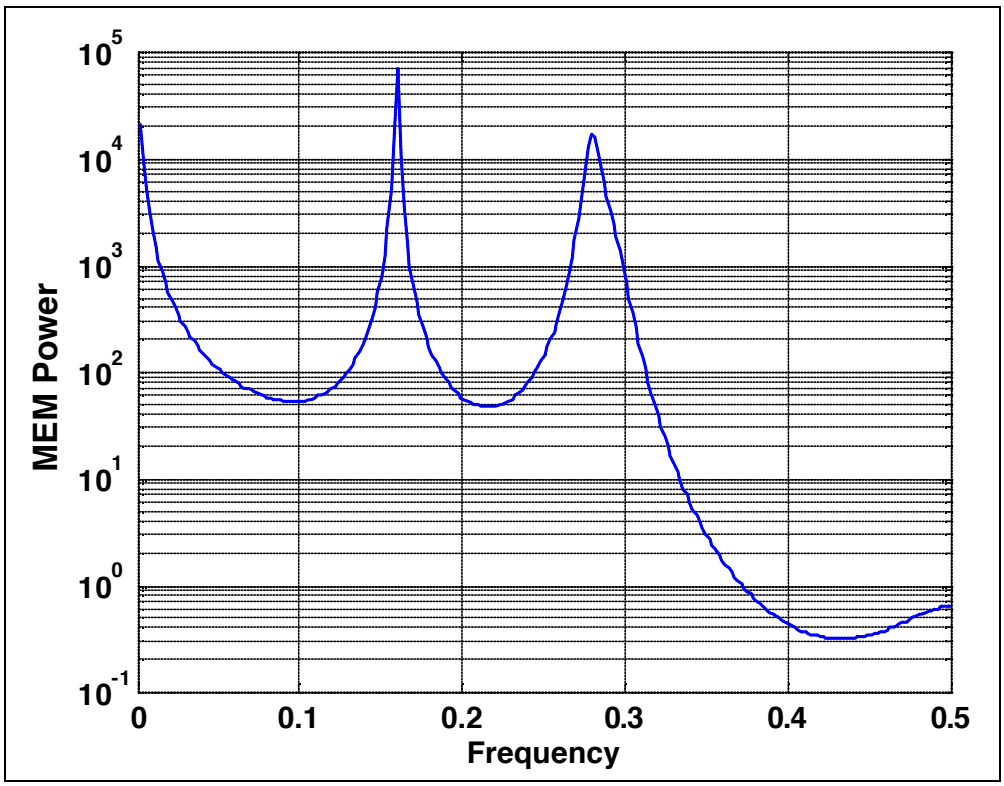

Figure 3.- Maximum entropy method (MEM) spectral estimates of the RC associated to the first 5 components of the annual time series of Uruguay River.

4. Results

4.1 Annual series

Mean and standard deviation of monthly streamflow are presented in Fig. 4 (left panels). It is noticeable that the relative variability of monthly discharges diminishes from east to west in LPB. For Negro River the standard deviation is larger than the mean during half of the year (December-May) while, on the other hand, for Paraná River the monthly mean is between 2.5 and 3.6 times the corresponding standard deviation. The annual accumulated discharge time series for the three rivers are shown in Fig. 4 (right panels).

SSA-MC, MEM and MTM were applied to the Negro, Uruguay, Paraná, N3.4, and PDO annual series. The results obtained by the three methods are essentially consistent and are shown in Table 2 and depicted in Fig. 5. The most robust multi-annual signals correspond to pseudo-periods in the range from 3 to 6 years, typically pertaining to the El Niño-Southern Oscillation (ENSO) timescales. The most conspicuous mode is the one associated to around 3.6 years. The three rivers also show significant LFV components associated to time scales longer than 30 years. There does not seem to be any clear link to the PDO signal and it is noticeable that no specific pseudo-periods longer than 10 years are detected by any of the three methods. Although Robertson and Mechoso, 1998, considered time series of paired rivers (see Section 1), most of the quasi-cycles found here are concordant with theirs.

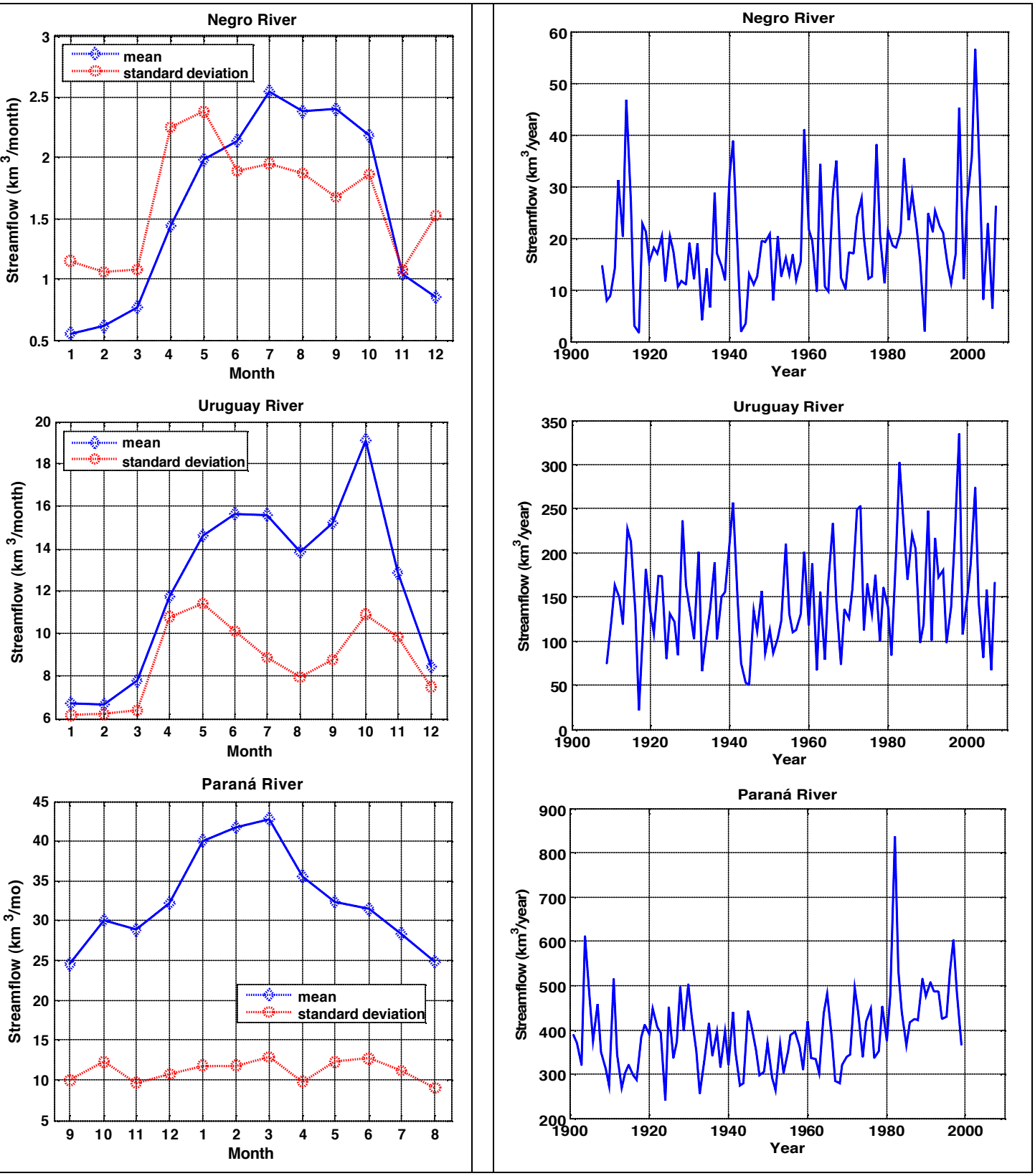

Figure 4.- Mean and standard deviation of monthly streamflow (left), and accumulated annual time series (right) for the three rivers in this study.

Table 2.- Pseudo-periods (in years) and low frequency variability modes (LFV) associated to annual series. For the three rivers and Niño 3.4, window sizes (M) of 15, 20 and 30 years were used for SSA-MC, while 20, 30 and 35 years were used for PDO. The dominant pseudo-periods or LFV modes shown in the second column were determined adjusting a sinusoid to the corresponding EOF as stateed in Section 3. The significance levels attained by the corresponding components according to the MC test are also shown in the second column (in brackets). Only results with at least 90% significance level are presented. Bold characters indicate that the significance level is reached for two values of M, and bold plus underlined characters are used when the significance level is attained by the three values of M. Pseudo-periods detected by MEM for significant components according to MC are shown in the third column. In the fourth column, pseudo-periods captured by MTM and the exceeded significance level (in brackets) are shown.

	SSA-MC	SSA-MEM	MTM
Negro	**3.6** (90%) 8.7 (90%) 9.1 (90%)	**3.6** **8.9** LFV	3.6 (99%) 2.3 (95%) 5.6 (90%) 8 (90%)
Uruguay	**3.6** (90%) **LVF** (90%) **6.3** (90%)	**6.2** **LFV** **3.6**	3.6 (99%) 6.4 (95%) 2 (95%) LFV (90%)
Paraná	**LFV** (90%) **3.6** (96%)	**LFV** **3.6** 3.4	3.6 (99%) 2.4 (99%) 7.8 (95%) LFV (90%)
Niño 3.4	**5.4** (98%) 3.6 (96%)	**5.6** 3.6 5	5.3 (99%) 3.6 (95%)
PDO	**5.7** (90%) **2.2** (90%)	**5.7** **2.2** **23** 3.2	5.4 (99%) 2.1 (95%) 3.2 (90%)

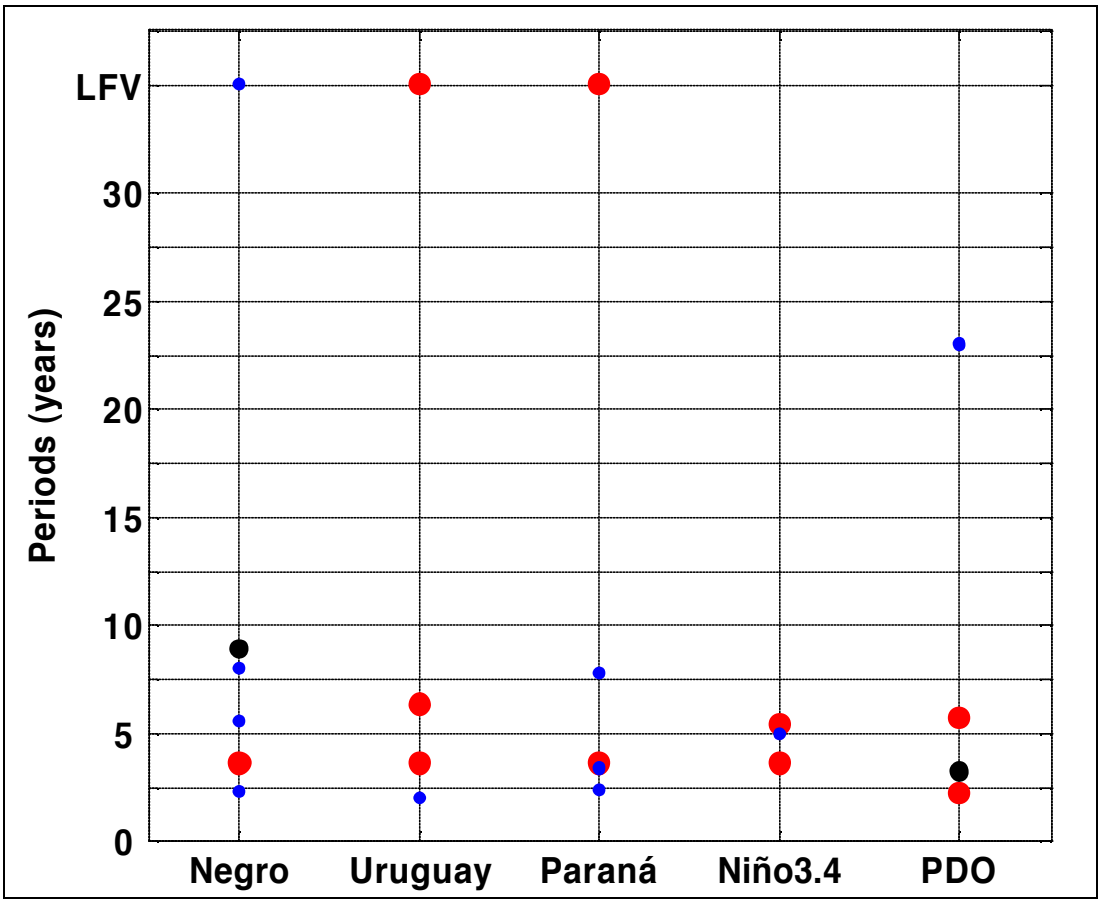

Figure 5.-Pseudo-periods and LFV modes for annual series obtained by SSA-MC, SSA-MEM and MTM (see Table 2). Bullets indicate, in decreasing order of size, whether the pseudo-periods were obtained by the three, two, or only one of the methods.

Table 3.- For annual time series, percent of explained variance by RCs associated to components with a SSA-MC significance level larger than 90 %, and the components that build each RC (in brackets). Windows size of M=20 years and M=30 years were used for rivers and global indices, respectively.

Annual series	% of variance explained by the reconstructions
Negro	25.4 Reconstruction associated with components: (1, 2, 3, 4)
Uruguay	34.9 (1, 2, 3, 4, 5)
Paraná	29.2 (1, 5, 6)
Niño 3.4	26.4 (1, 2, 3, 4)
PDO	8.6 (3, 5, 14, 18)

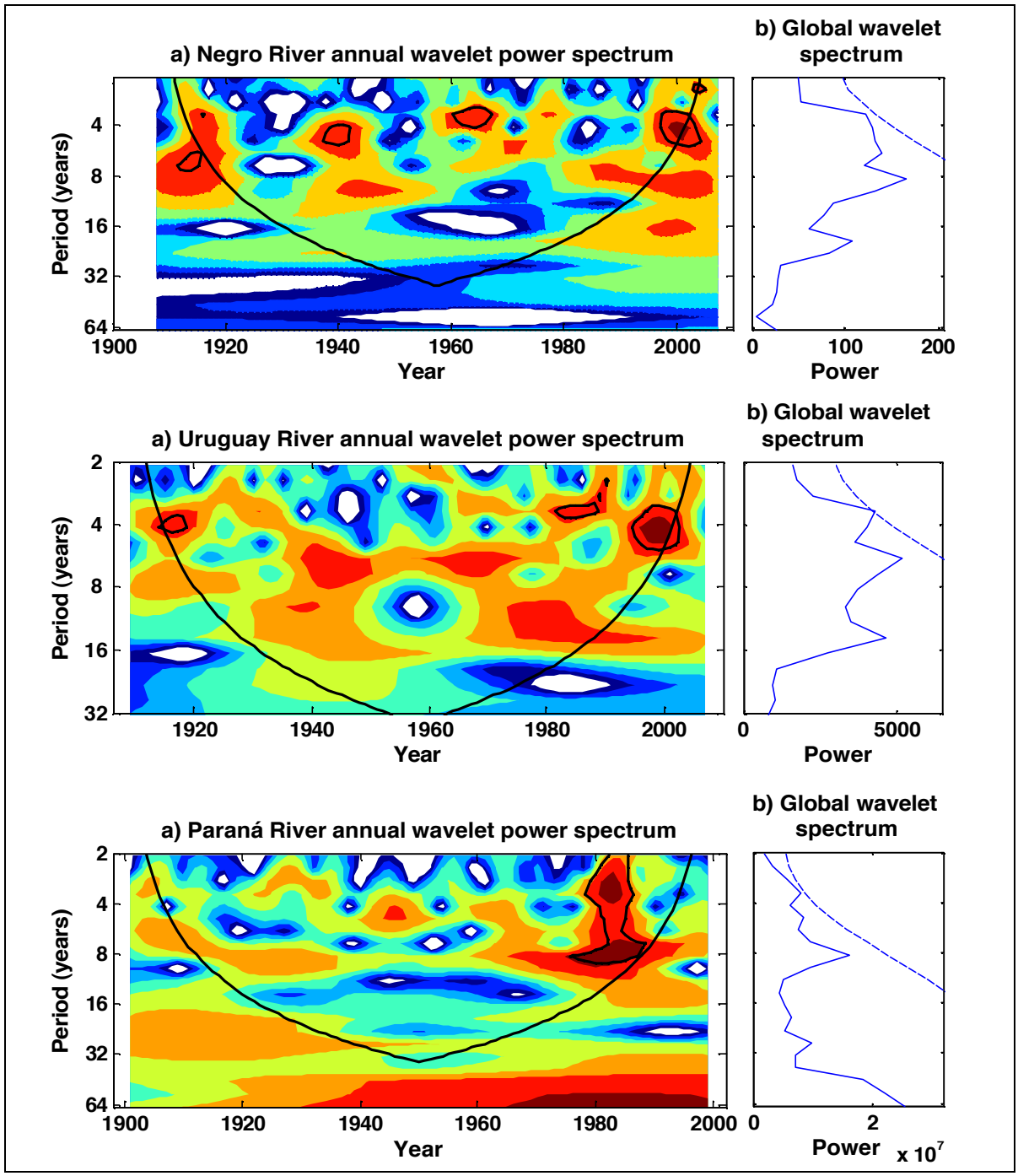

Figure 6.- Wavelet power spectra (left) and global wavelet spectra (right) for annual time series of rivers. Morlet wavelet is used. Red (blue) regions indicate higher (lower) power values. Black contours denote 95% significance level. The black thin curve is the cone of influence. Values in regions outside it are less reliable.

The percent of variance explained by RCs built based on significant components is shown in Table 3. It can be seen that, for rivers, it ranges from 25 % to 35 %, and that between 3 and 5 components participate in the RCs. It is worth mentioning that, for calendar years, the correlations between RCs associated to pseudo-cycles of 3.6 years for Uruguay, Paraná and N3.4 range from 0.67 to 0.70.

The results from Fig. 5 can be compared with those obtained by WA (see Fig. 6). It should be considered that WA allows determining the temporal variation of the spectral power of a given period.

For example, for Negro River (Fig.6, upper panel), significant wavelet powers appear intermittently along the record. The associated periods vary from around 8 to 4 years, in good agreement with pseudo-periods obtained by MEM and MTM (Fig. 5). The WA results for Uruguay and Paraná rivers are also consistent with the corresponding ones shown above. When we consider the global wavelet spectrum (i.e., the time average of wavelet spectra for a given period), we can see that only the 3.4-3.7 year period is significant at the 95 % level for Uruguay River, while it is marginally significant for the other two rivers. Note that, as indicated by the cone of influence, variability associated to time scales longer than 30 years is not captured by this method due to the length of time series.

4.2 Seasonal series

The question arises on what patterns of multi-annual variability are present during the annual cycle. In order to address this issue, SSA-MC and SSA-MEM were applied to the series of the 12 overlapping three-month periods for the 3 rivers. The results of this exercise are shown in Table 4. Figs. 7 to 9 depict the results of SSA-MEM for trimesters and annual series for Negro, Uruguay and Paraná rivers, respectively.

For Negro River (Fig. 7), dominant quasi-periods between 2.5 and 6 years occur mainly during the second half of the year, the most robust ones increasing from 3.5 years since JJA up to 5 years in DJF. Isolated modes appear associated to around 8.5 years in early winter, and to 2.2 years in spring. The former seems to have enough strength to build up the annual mode. LFV modes arise during late spring and summer (NDJ to JFM).

For Uruguay River (Fig. 8), dominant modes occur in winter and spring (6 years), summer and autumn (LFV). Two and 3.5-year pseudo-periods are also present, the former concentrated in late autumn and winter, and the latter in spring , although it shows weakly in autumn.

For Paraná River (Fig. 9), the most outstanding pattern of multi-annual variability is the appearance of LFV modes persisting from autumn to early summer (AMJ to NDJ), that will be analyzed later. The pseudo-cycles associated to 3.5 years are present in the second semester of the calendar year. In MAM and JAS, weaker and isolated modes around 5 years appear.

As in the case of annual time series, no specific quasi-cycles larger than 10 years are obtained for any of the rivers at any trimester.

Table 4.- Pseudo-periods (in years) and LFV modes of three-month time series for the three rivers obtained using two methods. For each trimester, in the first column: SSA-MC was applied for M=20; only results with at least 90% significance level are presented. In the second column, pseudo-periods detected by applying MEM to MC significant components (90%) are presented; results are ordered according to decreasing spectral powers of the associated peaks.

	JFM		FMA		MAM		AMJ		MJJ		JJA		JAS		ASO		SON		OND		NDJ		DJF	
	SSA MC	SSA MEM	SSA MC	SSA MEM	SSA MC	SSA MEM	SSA MC	SSA MEM	SSA MC	SSA MEM	SSA MC	SSA MEM	SSA MC	SSA MEM	SSA MC	SSA MEM	SSA MC	SSA MEM	SSA MC	SSA MEM	SSA MC	SSA MEM	SSA MC	SSA MEM
Negro	LFV (95%)	LFV	3.6 (90%)	3.5 6.2	None	None	None	None	6.3 (90%) 8.6 (90%)	6 8.3 3.5	3.5 (99%) 9.3 (99%) 7.2 (90%)	3.5 8.7 6.1	3.5 (98%)	3.5	3.7 (95%)	3.8 3.5	3.8 (90%) 2.3 (90%)	3.8 2.3 LFV	2.3 (90%) 3.9 (90%) 5.6 (90%)	3.9 2.3 5.7	LFV (92%) 5.1 (90%)	4.9 LFV 5.6 3.8	5.1 (95%) LFV (90%) 3.4 (90%)	5.1 LFV 3.4
Uruguay	LFV (95%)	LFV	LFV (95%)	LFV	LFV (90%)	LFV 9.3 3.5	2.2 (92%)	2.2 8.7 3.5	2 (90%)	2	2 (95%)	2 6	6.1 (95%)	6.2	6.3 (98%)	6.3	3.6 (92%)	3.7 6.3 2.5	None	None	2.4 (90%)	LFV 2.4 3.6	LFV (95%)	LFV
Paraná	None	None	None	None	5 (90%)	5.2 4.8	LFV (90%)	LFV	LFV (97%)	LFV	LFV (96%)	LFV	LFV (95%) 3.6 (90%)	LFV 3.7 4.9	LFV (97%) 3.6 (90%)	LFV 3.7 6.8	LFV (99%) 3.6 (99%)	LFV 3.6	LFV (99%) 3.6 (99%)	LFV 3.5	3.6 (95% LFV (95%)	LFV 3.5 3.7	None	None

It is interesting to note that some rivers present a similar and persistent multi-annual variability pattern during part of the annual cycle (e.g, Paraná River series for May-December, as revealed by Fig. 9). In order to pursue this item, time series showing a pseudo-period or LFV modes persisting for several trimesters were selected to analyze their preferred modes of variability. The series covering the remaining months were analyzed too (e.g., January-April for Paraná River). The results are shown in Table 5. They are consistent with those in Table 4, and those related to LFV will be further analyzed in the next subsection.

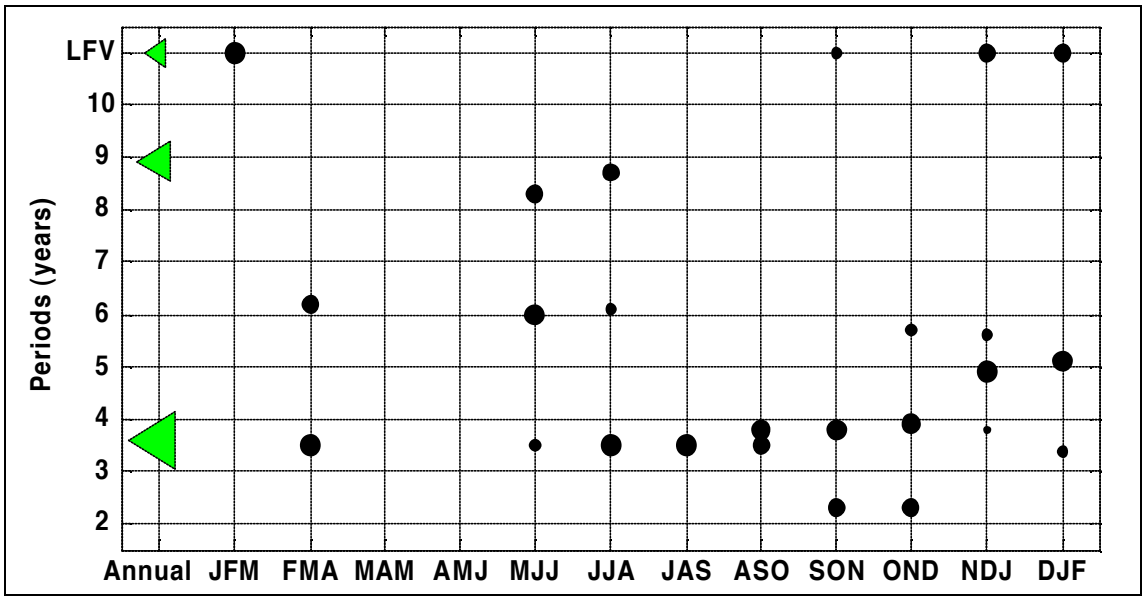

Figure 7.- Pseudo-periods and LFV modes obtained by SSA-MEM (see Table 4) for three-month and annual series of Negro River. Bigger symbol sizes indicate larger spectral power of a pseudo-period (circles) or LFV mode (triangles) than others at the same column.

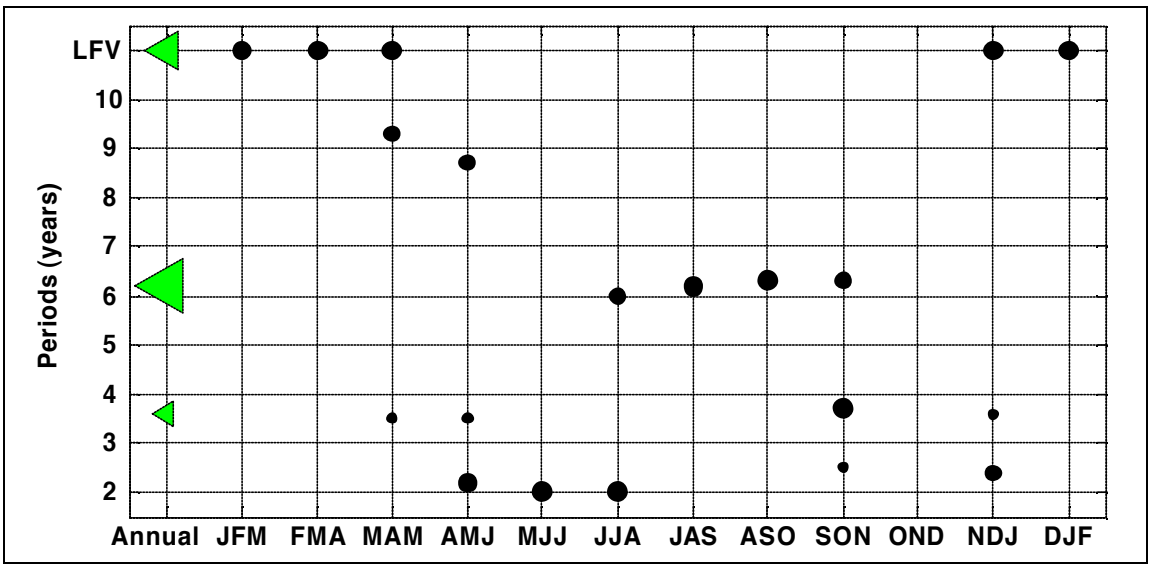

Figure 8.- Same as figure 7 but for Uruguay River.

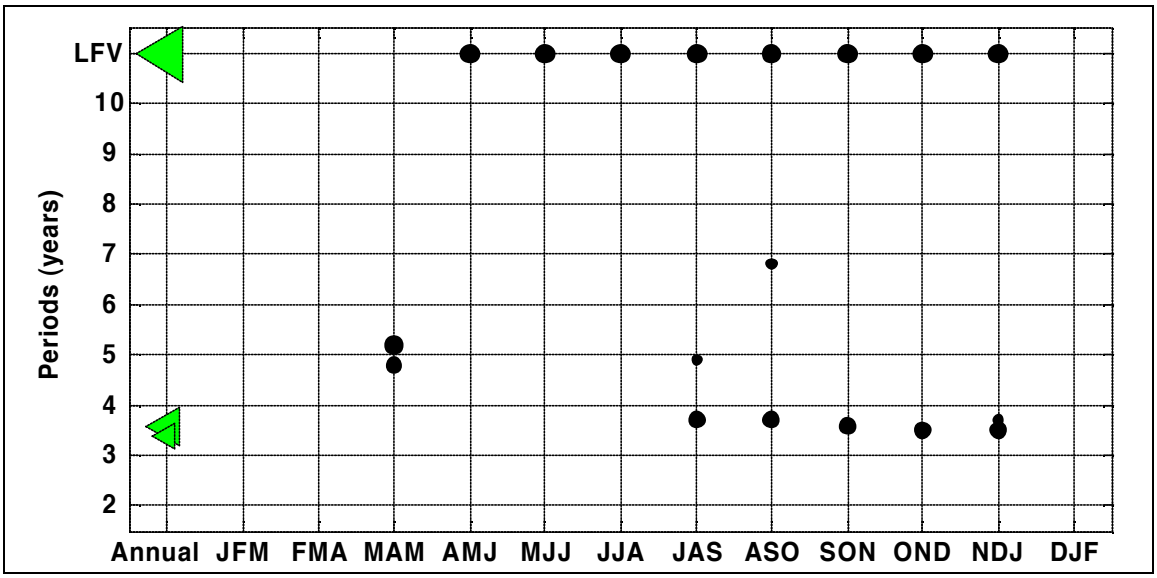

Figure 9.- Same as Figure 7 but for Paraná River.

Table 5.-Pseudo-periods (in years) and LFV modes of streamflow time series of the three rivers for selected periods (first column in each case) obtained using two methods. SSA-MC was applied for M=20 and M=30; bold characters indicate that the mode is captured using both window sizes. In the second column for each river, MC significance levels (larger than 90 %) are presented. Results in the third columns are obtained by applying MEM to MC significant components (90 %).

Negro series	SSA-MC	SSA-MEM	**Uruguay series**	SSA-MC	SSA-MEM	**Paraná series**	SSA-MC	SSA-MEM
Dec-Feb	**5.1** (95%) **LFV** (90%) 3.4 (90%)	**5.1** **LFV** 3.4 2.3	Dec-April	**LFV** (98%)	**LFV**	May-Dec	**LFV** (98%) **3.6** (98%)	**LFV** **3.7** 8.5 **3.5**
March-Nov	**3.6** (95%) **8.8** (90%) 2.3 (90%)	**8.8** **3.6** 2.3	May-Nov	**6.2** (95%) **3.6** (95%)	**6.2** **3.6**	Jan-April	**None**	**None**
June-Jan	**3.5** (92%) 2.3 (90%)	**3.5** 8.8 4.7 5.1 2.3	July-Oct	**6.3** (99%) 3.6 (90%)	**6.2** 3.6	Aug-Dec	**LFV** (99%) **3.6** (99%)	**LFV** **3.6**
Feb-May	LFV (90%)	LFV	Nov-June	**LFV** (97%)	**LFV**	Jan-July	**None**	**None**

4.3 Low frequency variability modes

In the previous subsections, one of the most prominent signals detected for the three rivers, both on the annual and seasonal bases, has been that of the long term variability (i.e. timescales longer than 30 years). We describe here the main features of these modes, given their relevance especially in the context of climate change.

First, we search for the existence of monotonic trends in annual raw streamflow time series (see Fig. 4 (right panels)). The results are shown in Table 6 (left). The three rivers exhibit increasing trends, being highly significant for Negro and Paraná, and marginally significant for Uruguay. These results are consistent with those of earlier studies (Genta et al., 1998, Berbery and Barros, 2002). Trends were also investigated for river time series selected according to results of Figs. 7 to 9 (see Table 6 (right)).

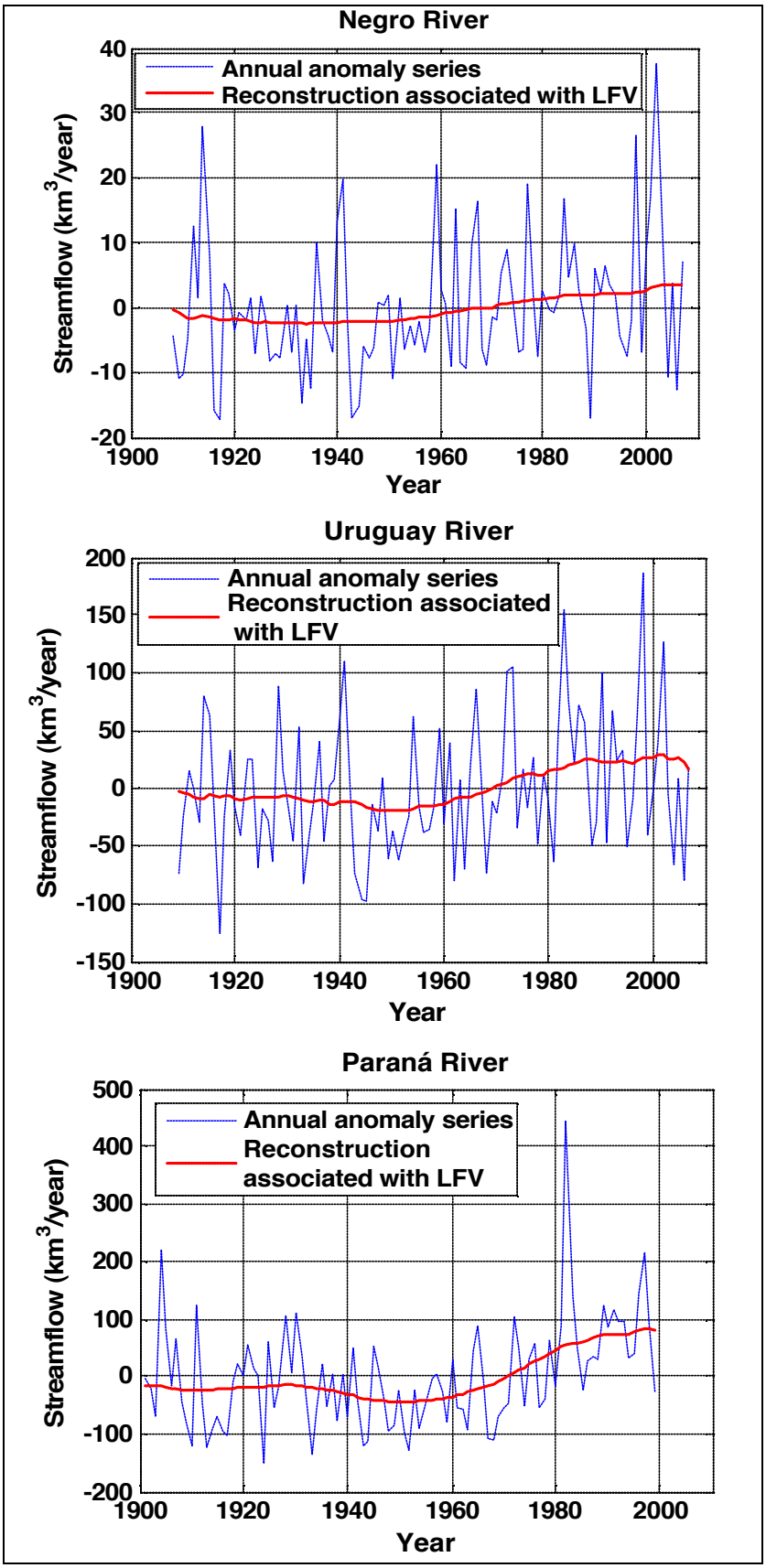

Figure 10.- Annual anomaly series and RC associated to LFV components.

Table 6.- Significance levels obtained by applying a Kendall-Mann test to: annual time series of rivers and global climate indices (left), and river time series (right) selected according to results of Figs. 7 to 9. Plus (minus) sign indicates increasing (decreasing) tendency.

Negro River	99.0 %
Uruguay River	93.9 %
Paraná River	99.9 %
Niño 3.4	2.2 %
PDO	-16.0 %

December-February (Negro)	98.87 %
March-November (Negro)	94.30 %
December-April (Uruguay)	98.62 %
May-November (Uruguay)	65.60 %
May-December (Paraná)	99.98%
January-April (Paraná)	44.04 %

LFV components for the annual time series of the rivers are presented in Fig. 10 together with the raw anomaly time series. It is apparent that, for the three cases, the long-term modes present a slight minimum in the 50's and, since then, they show a steady increase up to almost the end of the record, when there is a weak decrease. The percent of variance explained by components associated to LFV modes for each river are: 6.8 % for Negro River, 10.9 % for Uruguay River and 19.5 % for Paraná River.

The LFV modes associated to seasonal streamflow series also show interesting aspects. For Negro River, this signal is restricted to summer. For Uruguay River, we consider December-April, and for Paraná River, we focus on May-December (see Figs. 11, 12 and 13). For the three rivers, each LFV component was normalized by the variance of its own original series, allowing a fair comparison among the components. For each selected season, an increasing trend is evident (see first panels). For all the rivers, negative anomalies dominate from the beginning of the record up to the 60's or 70's, while for the rest of the period an increasing pattern appears, being especially strong for Paraná. This river also shows the largest percents of explained variances, followed by Uruguay River. It can also be seen that, for Uruguay and Paraná the maximum variance is reached in the middle of the selected season. For the Paraná River, it is striking that for all the 8 trimesters since AMJ up to NDE, LFV modes are associated to the first (and significant) eigenvalue.

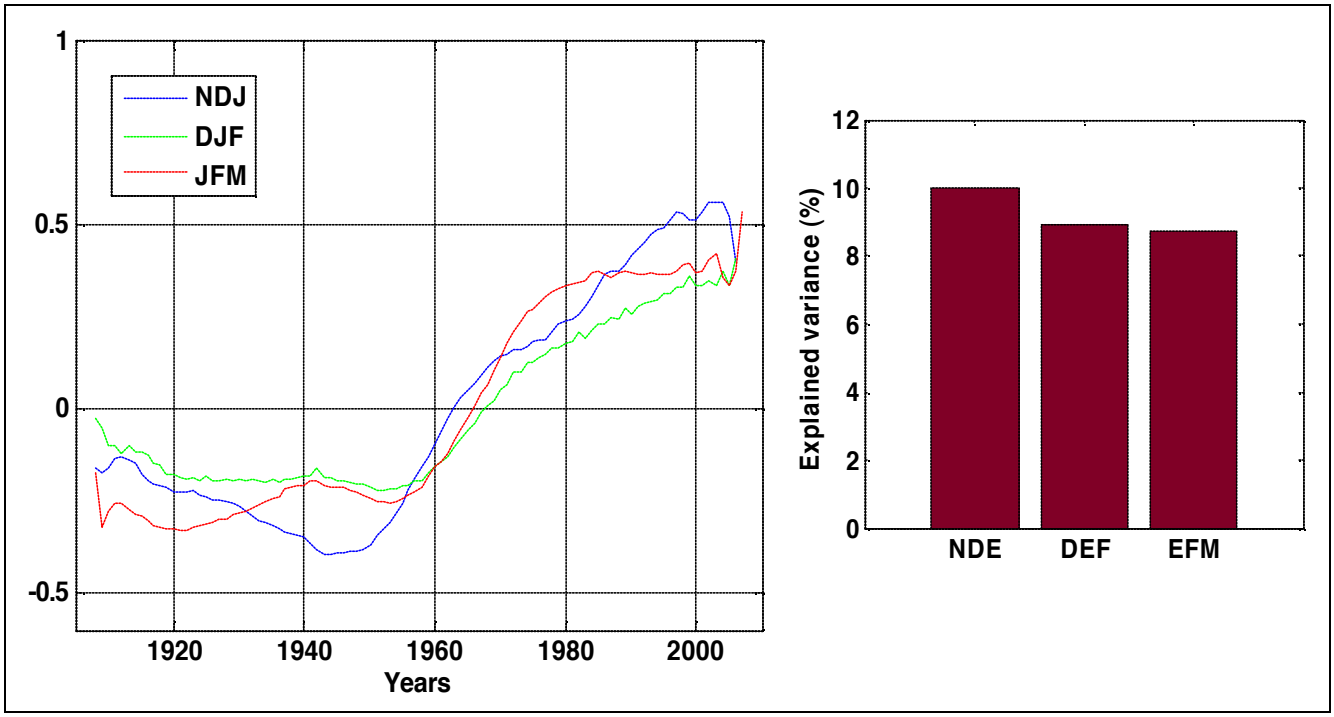

Figure 11.- Non-dimensional LFV components of selected three-month streamflow time series of Negro River. DJF and JFM are filtered (left panel). Percent of explained variance by each three-month LFV component (right panel).

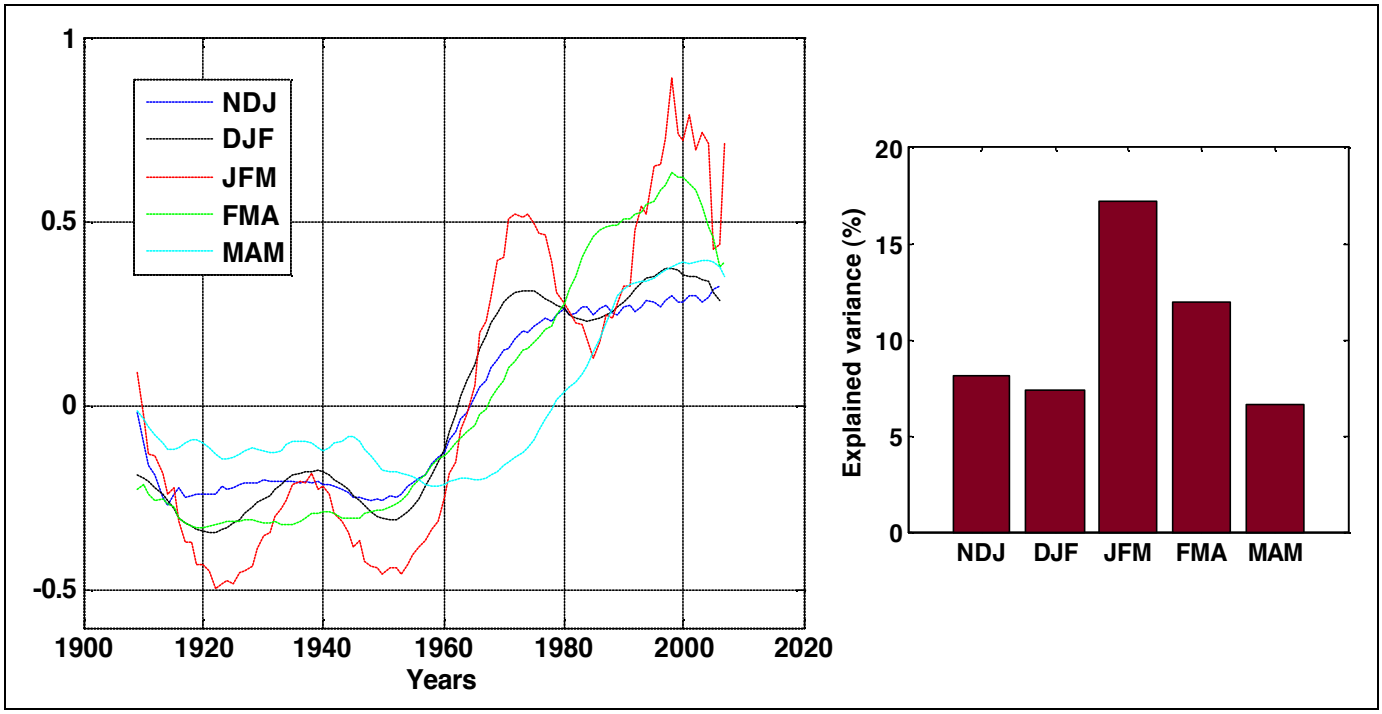

Figure 12.- Same as Fig. 11 but for Uruguay River. NDJ and MAM components are filtered.

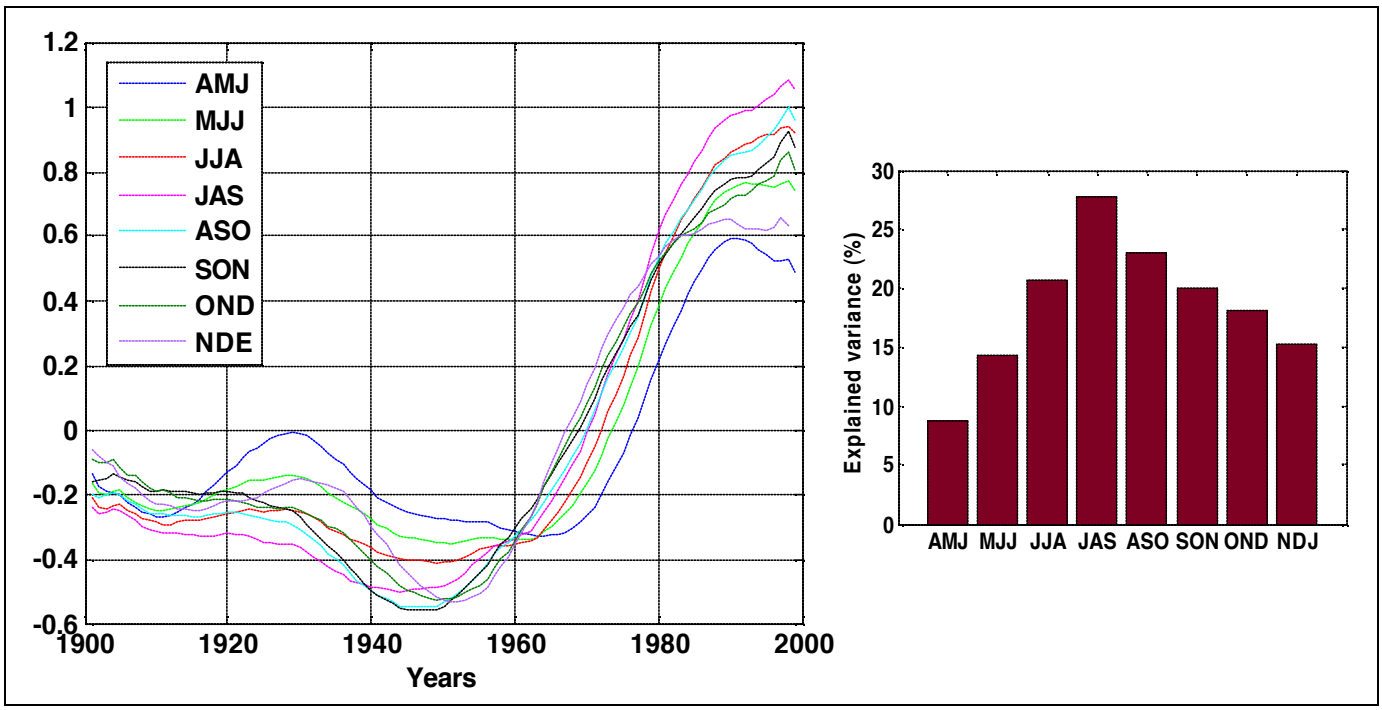

Figure 13.- Same as Fig. 11 but for Paraná River. All components are associated to the corresponding first eigenvalue obtained using SSA with M=20. No components are filtered.

5. Conclusions

The following are the main conclusions obtained from this study:

- Streamflow variability in LPB presents a strong link with ENSO, in pseudo-periods between 3 and 6 years approximately. In particular, there is a pervasive signal of 3.5 years both for annual and seasonal time series of the three rivers.
- Pseudo-cycles of 8-9 years appear in Negro and Uruguay rivers either in annual or seasonal time scales.
- No quasi-periods above 10 years are obtained either for annual or seasonal time series, the exception being PDO time series, which exhibits a weak quasi-period of 23 years.
- No specific relationship between PDO and river discharges in LPB is apparent.
- For the annual series, the three rivers show significant low frequency components, associated with long term (above 30 years) variability. For Uruguay and Paraná an increasing trend is evident beginning in the 60´s, with a weak decreasing tendency in the last few years of the record, while for Negro river there is a clear increase during the whole period, but it is less robust.
- Preferred modes of multiannual variability present a clear seasonality. Negro River shows its increasing trend in the summer. The most salient signal is that of Paraná River, that exhibits LFV modes associated to increasing trends between May and December. For Uruguay River the increasing trend is observed during the December-April period. Note that both periods cover the whole annual cycle, giving rise to complementary behaviours in the timing of trends of these two rivers. Another noticeable point is that, for the three rivers, the most intense increasing trend (as given by explained variance) coincides with the time of the minimum streamflow in the annual cycle (Figs. 11 to 13, right panel, and Fig. 4, left panels).

6. Acknowledgments

We have used the SSA-MTM Toolkit for Spectral Analysis, distributed by the SSA-MTM Group, Department of Atmospheric Sciences, University of California, Los Angeles (http://www.atmos.ucla.edu/tcd/ssa/).

7. References

Berbery, E. H. and V. R. Barros (2002). The Hydrologic Cycle of the La Plata Basin in South America . *Journal of Hydrometeorology*, 3, 630-645.

Genta, J. L., G. Perez-Iribarren, and C. R. Mechoso (1998). A recent increasing trend in the streamflow of rivers in southeastern South America. *J. Climate,* 11, 2858-2862.

Ghil, M., M. R. Allen, M. D. Dettinger, K. Ide, D. Kondrashov, M. E. Mann, A. W. Robertson, A. Saunders, Y. Tian, F. Varadi and P. Yiou (2002). Advanced spectral methods for climatic time series . *Reviews of Geophysics*, 40(1), doi: 10.1029/2001RG000092.

Labat, D. (2008). Wavelet analysis of the annual discharge records of the world's largest rivers . *Advances in Water Resources*, 31, 109-117.

Mann, M. E. and J. M. Lees (1996). Robust estimation of background noise and signal detection in climatic time series . *Clim. Change*, 33, 409-445.

Robertson, A. W. and C. R. Mechoso (1998). Interannual and Decadal Cycles in River Flows of Southeastern South America . *Journal of Climate*, 11, October 1998, 2570-2581.

Torrence, C. and G.P. Compo (1998). A Practical Guide to Wavelet Analysis . *Bulletin of the American Meteorological Society*, 79, 61-78.

Vautard, R., P. Yiou and M. Ghil (1992). Singular-spectrum analysis: A toolkit for short, noisy chaotic signals *Physica D*, 58, 95-126, North-Holland.